



HAL
open science

Stainless steel coated with carbon nanofiber/PDMS composite as anodes in microbial fuel cells

Meriem Saadi, Julien Pézard, Naoufel Haddour, Mohsen Erouel, Timothy M.
Vogel, Kamel Khirouni

► To cite this version:

Meriem Saadi, Julien Pézard, Naoufel Haddour, Mohsen Erouel, Timothy M. Vogel, et al.. Stainless steel coated with carbon nanofiber/PDMS composite as anodes in microbial fuel cells. *Materials Research Express*, 2020, 10.1088/2053-1591/ab6c99 . hal-03327537

HAL Id: hal-03327537

<https://hal.science/hal-03327537>

Submitted on 27 Aug 2021

HAL is a multi-disciplinary open access archive for the deposit and dissemination of scientific research documents, whether they are published or not. The documents may come from teaching and research institutions in France or abroad, or from public or private research centers.

L'archive ouverte pluridisciplinaire **HAL**, est destinée au dépôt et à la diffusion de documents scientifiques de niveau recherche, publiés ou non, émanant des établissements d'enseignement et de recherche français ou étrangers, des laboratoires publics ou privés.

PAPER • OPEN ACCESS

Stainless steel coated with carbon nanofiber/PDMS composite as anodes in microbial fuel cells

To cite this article: Meriem Saadi *et al* 2020 *Mater. Res. Express* 7 025504

View the [article online](#) for updates and enhancements.



IOP | ebooks™

Bringing together innovative digital publishing with leading authors from the global scientific community.

Start exploring the collection—download the first chapter of every title for free.

Materials Research Express



PAPER

Stainless steel coated with carbon nanofiber/PDMS composite as anodes in microbial fuel cells

OPEN ACCESS

RECEIVED

23 October 2019

REVISED

5 January 2020

ACCEPTED FOR PUBLICATION

16 January 2020

PUBLISHED

4 February 2020

Original content from this work may be used under the terms of the [Creative Commons Attribution 4.0 licence](#).

Any further distribution of this work must maintain attribution to the author(s) and the title of the work, journal citation and DOI.



Meriem Saadi¹, Julien Pézard², Naoufel Haddour² , Mohsen Erouel¹, Timothy M Vogel² and Kamel Khirouni¹

¹ Laboratory of Physics of Materials and Nanomaterials Applied at Environment, Faculty of Sciences in Gabes, Gabes University, 6072, Gabes, Tunisia

² Université de Lyon, Ecole Centrale de Lyon, UMR CNRS 5270, Ampère, F-69130 Ecully Cedex, France

E-mail: naoufel.haddour@ec-lyon.fr

Keywords: microbial fuel cell, CNF-PDMS, stainless steel electrodes, biofilm, extracellular electron transfer

Abstract

Modification of electrode surfaces is a promising strategy to improve microbial fuel cell (MFC) performance. Here we report a new functionalization process to improve interfacial electron transfer, biocompatibility and corrosion resistance of stainless steel (SS) electrodes used as anodes in MFCs. SS anodes prepared by surface modification with a thin layer (200 μm) of conducting composite made of polydimethylsiloxane (PDMS) doped with commercially available carbon nanofibers (CNF), are described. Electrochemical characterization showed that the corrosion rate of SS electrode in an acid solution decreased from 367 $\mu\text{m}\cdot\text{y}^{-1}$ to 31 $\mu\text{m}\cdot\text{y}^{-1}$ after CNF-PDMS coating. Electric characterization demonstrated that the maximum power density generated by MFCs after 16 days with SS/CNF-PDMS anodes (19 $\text{mW}\cdot\text{m}^{-2}$) is 5 times higher and more stable than that with unmodified SS (3.7 $\text{mW}\cdot\text{m}^{-2}$). The cyclic voltammetry analysis indicated that the electrochemical activity of the modified anode was enhanced significantly after 16 days and the electron transfer was facilitated by CNF-PDMS modification. Microscopic observations and electrochemical characterization showed that CNF-PDMS composite improved biocompatibility and corrosion resistance of the SS anode surfaces. These results confirmed that the CNF-PDMS modification is a promising approach to improve the properties of anode materials for MFC application.

1. Introduction

Microbial fuel cells (MFCs) have been recognized as a promising technology for the direct conversion of organic matter into electricity using bacterial biofilms as biocatalysts [1–3]. The possibility of producing electrical energy from organic waste with this technology opens up perspectives for renewable energy recovery from sewage, industrial effluents, and agricultural waste. Thus, this technology could have the dual advantage of producing clean, sustainable energy and eliminate waste. However, the electricity production of MFCs remains too low for their large-scale applications in wastewater treatment. These restrictions are mainly due to the slow kinetics of electron transfer from bacteria to electrode surfaces at anode electrode [4]. The electroactive bacteria are able to use the anode, which is made out of an electrically conductive material, as the final electron acceptor of their anaerobic respiratory chain. Electrons are thus released to the anode and then travel to the cathode through an external electrical circuit. The development of low cost and high performance anodes, is one of the key factors for practical implementation of MFCs. Carbon materials in different forms (paper, cloths, foam, fibers, felt, granules...) are generally used as anode electrodes in MFCs [5–8]. These biocompatible materials are resistant to corrosion but have low mechanical stability and low electrical conductivity [9, 10]. Since carbon materials offer less electrical conductivity than pure metal, most material used for electrical connection of anodes to the external circuit, are metallic (titanium, stainless steel or copper). Indeed, carbonaceous current collectors could be a source of potential loss and a metallic collector plate is the best way to reduce electron travel distance and contact resistance between electroactive bacteria and the external circuit [11]. Cheng *et al* showed power losses

and drop in potential distribution on the electrode surface arising from resistivity of carbon anode material and current collector configurations [12]. Generally, corrosion of metal material limits their use as anode in MFC application. SS has been proposed as alternative material for anode electrodes in MFCs due to its high conductivity compared to carbonaceous materials [13]. However, SS electrodes used as anodes in MFCs suffer from poor biocompatibility and corrosion fatigue [14, 15]. Several research groups have reported that SS surface modification succeeded in improving biocompatibility and corrosion resistance of SS anodes, as well increasing the power density produced by MFCs. Liang *et al* reported surface modification of SS electrodes by chemical vapor growth of carbon coat, by electrodeposition of polyaniline polymer, by electrochemical grafting of neutral red molecules and by heat treatment [16]. These studies showed the possibility of improving the power generation of MFCs with SS anodes but their corrosion resistance performance was not reported. Pu *et al* described electrochemical polymerization of polypyrrole on the surface of SS anodes [17]. Polypyrrole modification improved corrosion resistance and biocompatibility for a better MFC performance. However, some factors currently limit the applications of polypyrrole because of its low mechanical properties and low processibility [18]. The aim of this work is to study a new modification method of SS anode surfaces with thin layer (200 μm) of low-cost and mechanical stable CNF-PDMS composite. This new functionalization approach improves interfacial electron transfer, biocompatibility and corrosion resistance of anode surfaces, and ensures a homogenous potential distribution on the surface through the current collector configuration 'large plate metallic current collector'. In addition, the thin layer of CNF-PDMS carbon material reduces both travel distance between electroactive bacteria and the current collector, and the potential drop arising from resistivity of this carbon material. PDMS is a commercially available material with physically and chemically stable properties [19]. PDMS is an attractive material to fabricate microfluidic structures and is widely used for lab-on-a-chips. Recently, this elastomer was shown to be conductive after doping it with conducting nanoparticles and nanotubes [20–22]. Carbon doped PDMS was used in microfluidic systems for heating [23], detection of droplets [24], and electrochemical measurements [25]. However, the best of our knowledge, modification of SS electrodes with conducting PDMS was never reported even though these layers could be deposited on large electrode surfaces and at low costs.

2. Materials and methods

2.1. Electrode preparation

For CNF-PDMS preparation, we used a 10:1 (w/w) mixture of PDMS base and curing agent (Sylgard 182 Silicone Elastomer) that was degassed under vacuum. Carbon nanofibers (CNFs) with a diameter of 200 nm and length of 50 μm (purchased from Sigma-Aldrich, >99.9% carbon basis) were reinforced in insulating polymer (PDMS) at a weight ratio of 8:100 to prepare a conductive composite (CNF-PDMS). The mixture was thoroughly mixed for 20 min by hand until obtaining a homogeneous paste. SS foil of 0.25 mm thick (AISI 316L purchased from Goodfellow) was cut into square electrodes with dimensions of 1 \times 1 cm. SS electrodes were washed with acetone, ethanol and distilled water before using and then dried at room temperature. CNF-PDMS past was then cast on SS electrode surfaces and the obtained layer was levelled to the height of pattern placed around the electrode. SS modified electrodes were then cured 80 $^{\circ}\text{C}$ for 2 h. The thickness of the formed CNF-PDMS layer on the flat surface of the electrodes was controlled using a mechanical profilometer (Veeco Dektak 3030) and was around 0.2 mm high.

2.2. Electrode characterization

The morphology of the CNF-PDMS layers was examined with a scanning electron microscope (SEM, JEOL model JSM-7401 F). The resistivity of this material was determined by four-point measurements with a probe station and a Keithley 4200 Source Measure Unit (SMU). The corrosion resistance was investigated by Tafel curves using linear voltammetry in H_2SO_4 solution (0.1 M) at a scanning rate of 10 $\text{mV}\cdot\text{s}^{-1}$. A potentiostat OGS 100 from Orignalys was used to perform electrochemical characterizations. The unmodified and modified SS electrodes were used as working electrodes, a commercial saturated Ag/AgCl electrode as a reference and a Pt wire electrode as an auxiliary electrode. The geometric surface area of unmodified and modified electrodes was used for calculating both corrosion current density and power density of MFCs.

2.3. MFCs setup and operation

Single-chamber batch MFCs were set up in 250 ml Wheaton bottles realized by (Schott Duran, Germany) for laboratory applications. The air cathodes were made of carbon cloth Fuel (Cell Earth, Woburn, USA). Then were coated with PTFE and 5% of platinum catalyst as described by Cheng *et al* [26]. The cathode with a diameter of 2.3 cm was fixed by a clamp and silicone sealant on the aperture side of the bottle. Each anode was placed in the

Table 1. The typical of PDMS composites doped with different carbon particles.

Polymer	Conducting particles	carbon %(w/w)	Conductivity [S.m ⁻¹]	References
PDMS	Carbon nanotubes	10	100	[27]
PDMS	Black carbon	8	0	[20]
PDMS	Black carbon	25	10	[25]
PDMS	Carbon nanofibers	8	80	This study

center of each bottle. Anode and cathode were placed on opposite sides of the reactors and connected to the external circuit by titanium wires (Alfa Aesar, Karlsruhe, Germany).

2.4. Biofilm preparation

The MFCs were filled with 250 ml of primary effluent and 1.25 g (5 g l⁻¹) of dehydrated sludge from a Grand Lyon domestic wastewater treatment plant (Lyon, France) and fed with 0.25 g (1 g l⁻¹) of sodium acetate (Roth, Karlsruhe, Germany) as carbon source. All reactors were cultivated simultaneously at a stable ambient temperature. An external resistance of 1000 Ω is connected to the electrodes in order to shuttle electrons from the anode to the cathode.

2.5. MFCs operation

The MFC voltage was recorded every 5 min using an Agilent 34970 (a data acquisition instrument/Switch Unit) with a precision of 1 μV. MFC electrical performances were determined by polarization curve analysis using linear sweep voltammetry (LSV) technique. The LSV tests were carried out with potentiostat (origaflex 0GF01A, France) by potential sweep from open circuit potential (OCP) of the MFC to 0 V at a scanning rate of 1 mV.s⁻¹.

2.6. Biofilm characterization

The characterization of anodic biofilms was carried out by fluorescence microscopy. A LIVE/DEAD BacLight Bacterial viability kit (Invitrogen) was used to label the samples. 1.5 μl of propidium iodide and an aliquot (1.5 μl) of SYTO9 were mixed in 2 ml of sterile NaCl 0.8%. Thereafter, 200 μl were deposited on each sample of anodic biofilm and incubated for 15 min in the dark before observations with Axio Imager Zeiss microscope. The evolution of the biofilm electroactivity was measured 4 and 16 days after operation start by cyclic voltammetry (CV) with a rate of 10 mV s⁻¹ from -0.6V to 0.8V in a three electrode system. The anode was used as the working electrode, the cathode as the auxiliary electrode and an Ag/AgCl electrode was used as the reference electrode.

3. Results and discussion

3.1. Conductivity characterization of CNF-PDMS layers

Conductivity measurements showed that electrical resistance of CNF-PDMS layers saturated for samples containing more 8% mass ratio of carbon nanofibers to PDMS. We were unable to increase the conductivity of CNF-PDMS paste with higher carbon content because of mixing issues. For this ratio (8%), CNF-PDMS layers provided efficient electrical properties with a conductivity of (80 ± 1) S.m⁻¹ (table 1). This conductivity value was lower than the conductivity of carbon nanotubes/PDMS composites [27], but higher than that of the black carbon/PDMS composites previously described [15, 20]. Despite the low mass ratio of carbon nanofibers, these results show that CNFs were well dispersed in the PDMS matrix and preserved connections in the percolated CNF networks. However, conductivity of 316 L SS unmodified foil (1.33 × 10⁶ S.m⁻¹ according to supplier data) is around 104 times greater than CNF-PDMS conductivity.

3.2. Electrode surface morphology of C-PDMS coated anode

EM images show that CNFs are well dispersed and randomly oriented on the surface of the polymer (figure 1(A)). These results demonstrated that the deposition of CNF-PDMS on SS plate increases the effective surface area of the electrode. The high magnification micrograph (figure 1(B)) shows that the diameter of single nanofibers at the exit of the PDMS matrix is higher than the 200 nm indicated by the supplier. This part of the fibers, is coated with PDMS, which must reduce their surface conductivity. This is attributed to the strong linkage between nanofibers and polymer matrix that leads to a decoration of CNFs by polymer molecules. However, we note that the diameter of nanofiber extremities is around 200 nm (figure 1(C)), which corresponds to the value indicated by the supplier. This means that they are stripped and conductive. These comb-like conducting structures on CNF-PDMS layers could facilitate the direct extracellular electron transfer (EET) of

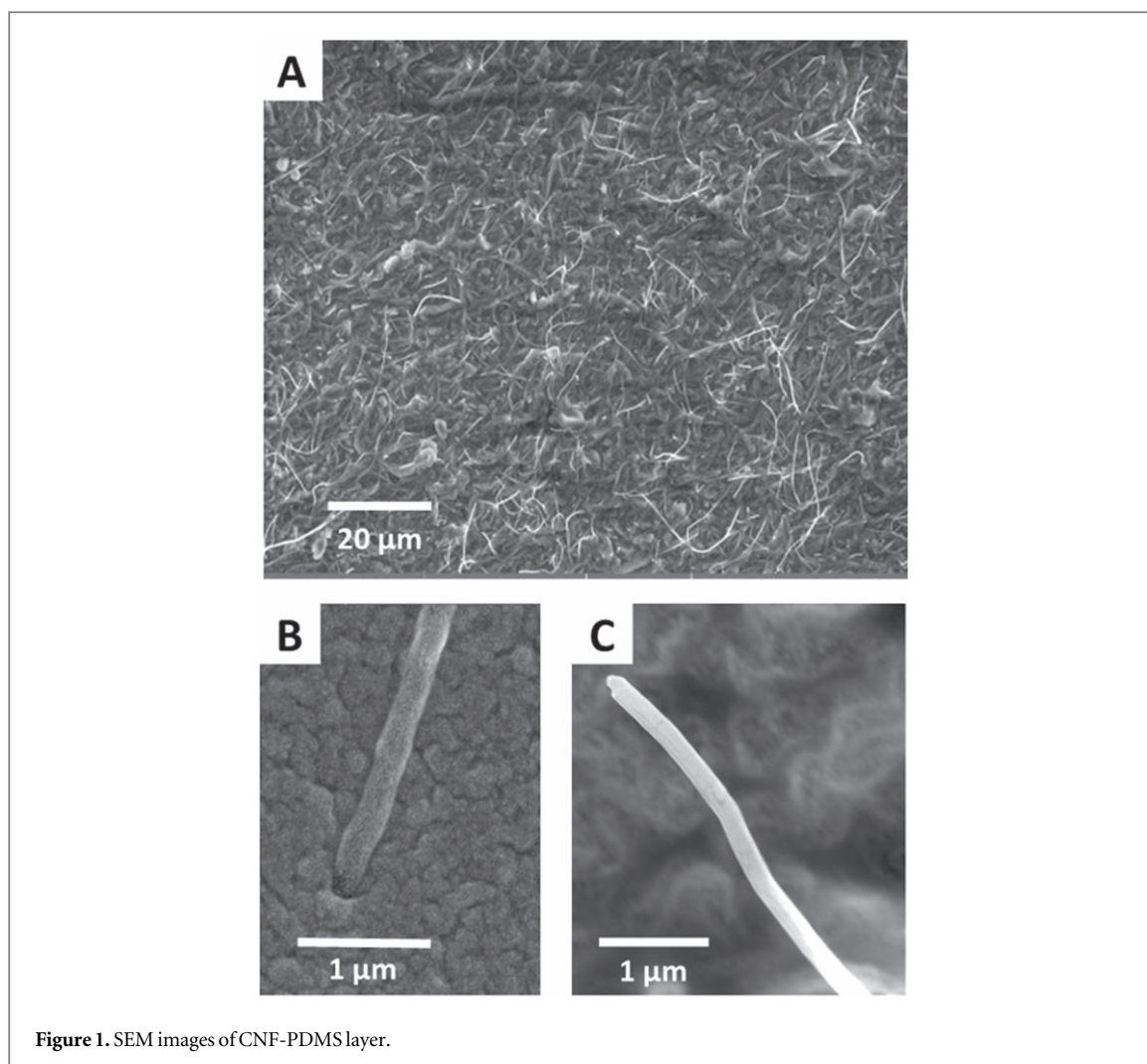


Figure 1. SEM images of CNF-PDMS layer.

electroactive bacteria (EAB) to the electrode. In direct EET, EAB (e.g., *Geobacter sulfurreducens*) can transfer their electrons directly via conductive pili called nanowires [28].

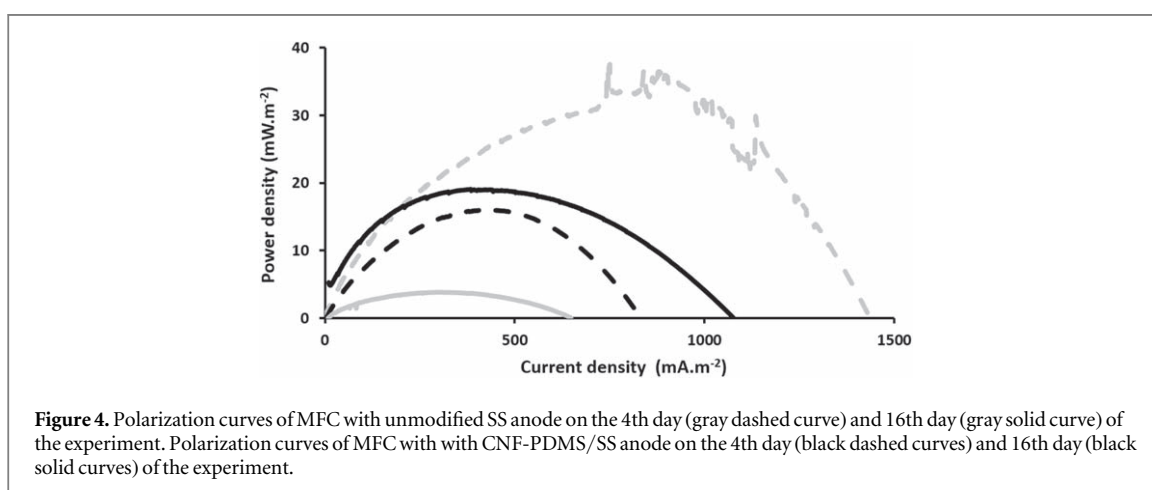
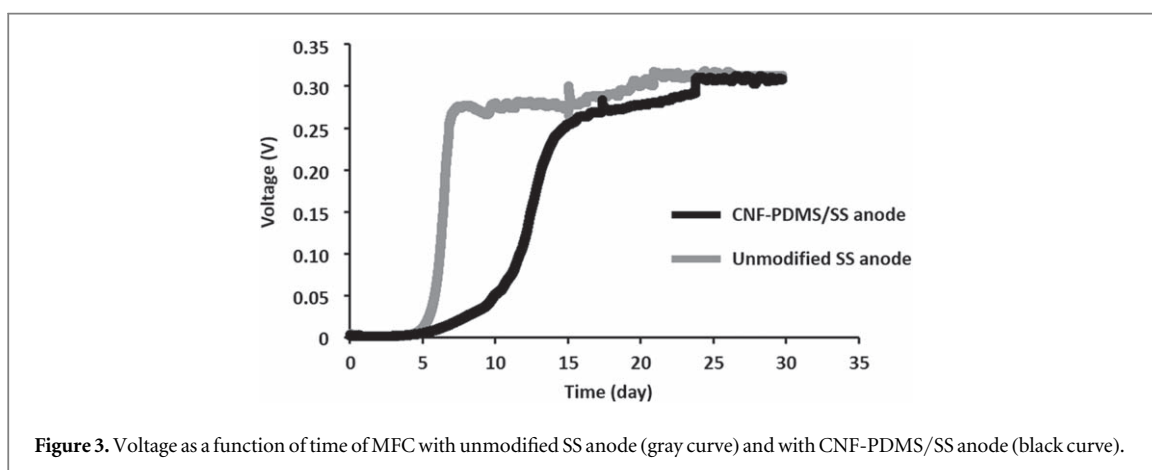
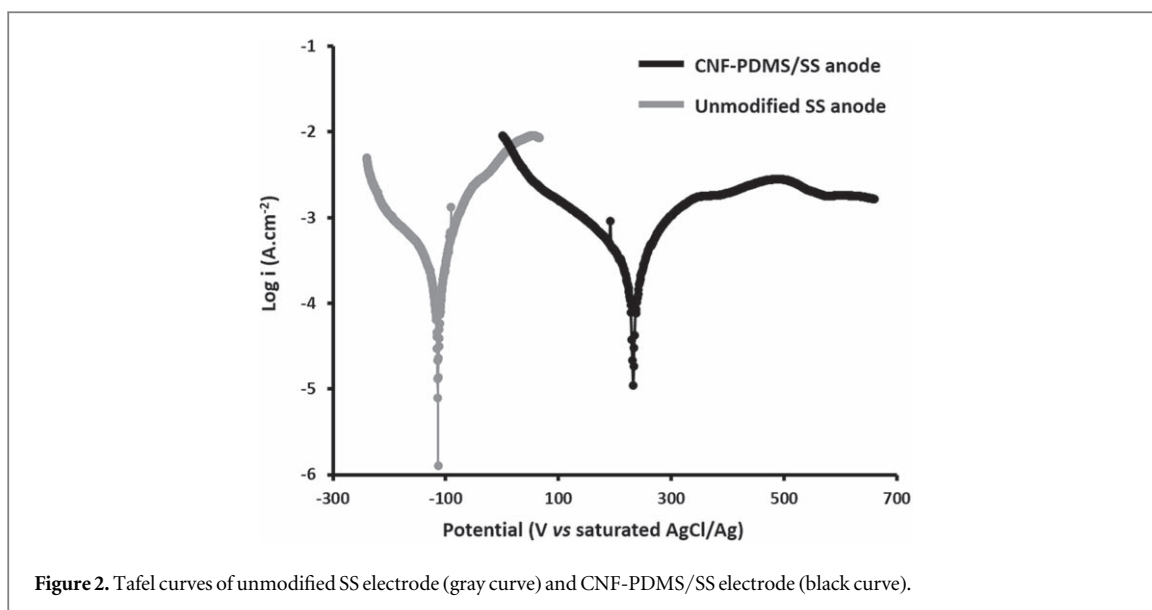
3.3. Anti-corrosion performance of C-PDMS coated anode

The Tafel curves of the unmodified and modified SS electrodes indicated that the corrosion potential increased from -113 mV to 232 mV and the corrosion current decreased from $2.1 \text{ mA}\cdot\text{cm}^{-2}$ to $0.17 \text{ mA}\cdot\text{cm}^{-2}$ after CNF-PDMS deposition on SS surfaces (figure 2). The decrease of corrosion current and the rise of the positive corrosion potential were consistent with a better anti-corrosion performance. The corrosion resistance of CNF-PDMS/SS electrodes was better than that of bare SS electrodes and the corrosion rate of SS electrode decreased from $367 \mu\text{m}\cdot\text{y}^{-1}$ to $31 \mu\text{m}\cdot\text{y}^{-1}$ after CNF-PDMS coating. These results ensure that CNF-PDMS layers have an anti-corrosion effect by preventing the direct contact between SS surface and solutions.

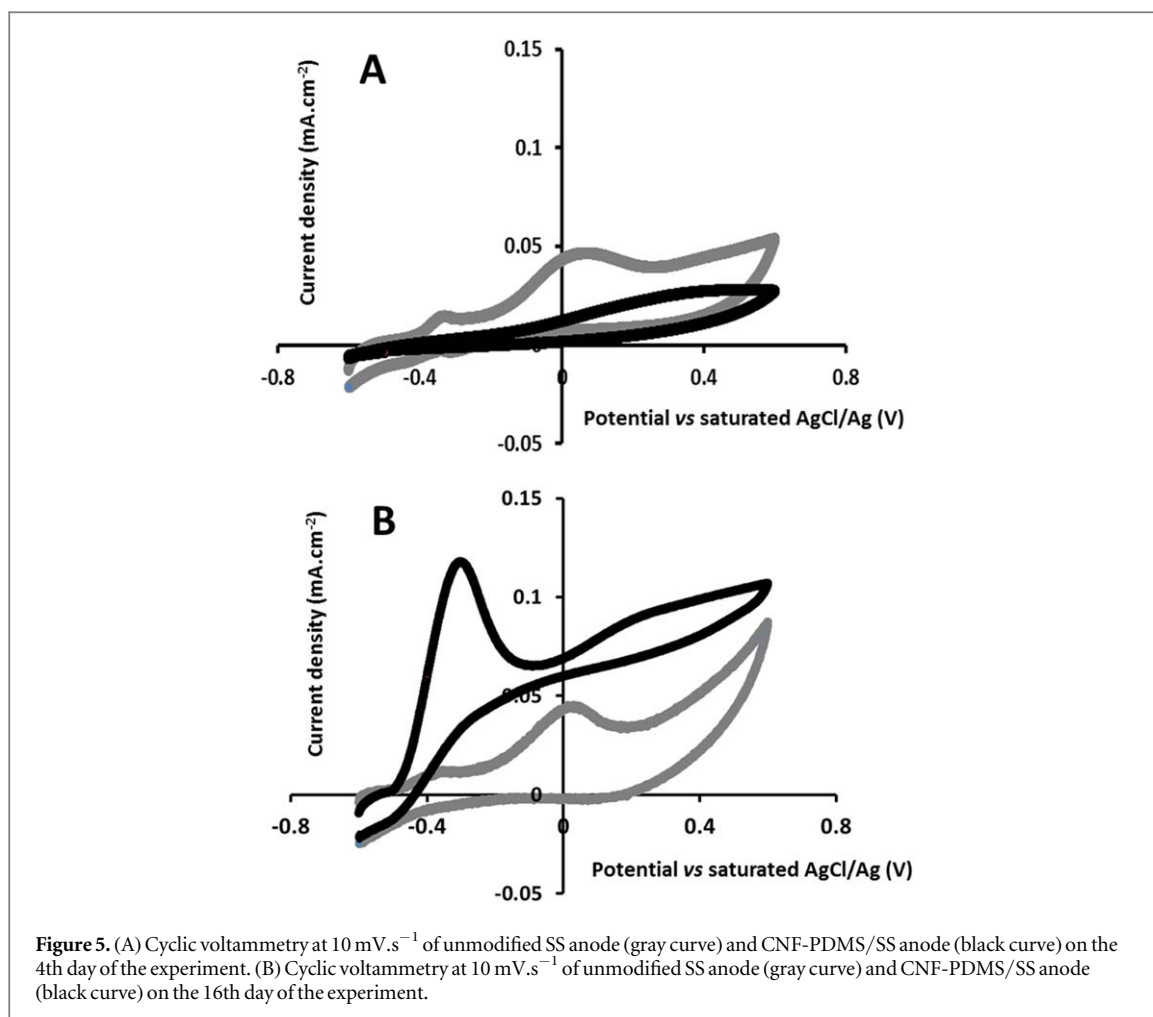
3.4. Electricity production performance

The MFC voltage was recorded as function of time during a month in order to follow the biofilm formation on anode surfaces. The voltage of MFC with unmodified SS anode increased rapidly on the 5th day of the experiment (5 days after inoculation of MFCs with primary effluent and domestic wastewater) reaching 0.26 V (figure 3).

The voltage of MFC with CNF-PDMS/SS anode progressively increased after a week and reached the same value after two weeks. These results indicate that the biofilm grows less well on the surface CNF-PDMS anode than that of unmodified SS anode. The startup time of MFC with CNF-PDMS anodes, was probably increased by the non-conductive part of the surface (PDMS) which is hydrophobic. Indeed, Santoro *et al* reported that hydrophobic surfaces slowed down the biofilm attachment and made the start-up period of MFCs longer [29]. Therefore, it is possible that this long start up period for CNF-PDMS surfaces is the result of the harder biofilm formation on this material.



The maximal power density of MFCs was measured at different times in order to compare the electroactivity of biofilms (figure 4). After 4 days, the maximal power density of MFC with unmodified SS anode (35 mW.m^{-2}) was almost twice as high as the maximal power density of MFC with CNF-PDMS/SS anode (16 mW.m^{-2}). This difference was probably due to the low conducting area of CNF-PDMS layers. The surface of this conductive polymer is composed in a large part of insulation and about 10% of conductive surface, unlike unmodified SS anodes where the entire surface is conducting. Although the conductive area of this composite surface only



corresponds to about 10% of its geometric surface and is almost 10 times smaller than the area of unmodified SS surface, the maximum power density produced is only 2 times lower. The conducting CNFs enhanced EET transfer between EAB and composite anode. After 16 days, polarization curves showed a decrease in the maximal power density of MFC with unmodified SS anode to $3.7 \text{ mW}\cdot\text{m}^{-2}$, while the maximal power density of MFC with CNF-PDMS/SS anodes increased slightly to $19 \text{ mW}\cdot\text{m}^{-2}$. The decrease in the power performance of unmodified SS anodes was due to the poor biocompatibility and corrosion fatigue of this material. The stability of the electrical performances of the modified anodes demonstrated that CNF-PDMS layers improved the biocompatibility and corrosion resistance of SS anode surfaces.

3.5. Characterization of active biofilm

Cyclic voltammograms of MFC anodes were recorded on 4th and 16th days of the experiment (figure 5). After four days, cyclic voltammogram of unmodified SS anode exhibited a small faradaic peak centered at -400 mV versus Ag/AgCl and a higher one at 40 mV versus Ag/AgCl. The observed peaks correspond to two different modes of EET and to two life-style modes inside electroactive biofilms. One group, represented by *Shewanella oneidensis*, capable of using a large range of electron acceptors and substrates and able to mediate indirect EET, and another group, represented by *Geobacter sulfurreducens*, capable of using a small range of electron acceptors and substrates and able to mediate direct EET. Based on previously reported values, the negative potential region corresponded to mediated electron transfer of *Shewanella oneidensis* and/or heterogeneous electron transfer of *Geobacter sulfurreducens* EAB [30, 31]. At positive potentials, the direct electron transfer was the major EET mechanism [32]. Cyclic voltammogram of CNF-PDMS/SS anode on the 4th day, showed a low electroactive activity with a small Faradaic peak in the high positive potential region (400 mV versus Ag/AgCl). After sixteen days, the electrochemical response of the unmodified SS anode did not change much with a decrease in the intensity of the redox peak in the negative potential region. However, catalytic electroactivity CNF-PDMS/SS anode greatly increased and had two intense peaks in both positive and negative potential regions. These results indicated that after biofilm growth, CNF-PDMS layer improved both the biofilm formation and the EET of EAB on the surface of SS electrodes.

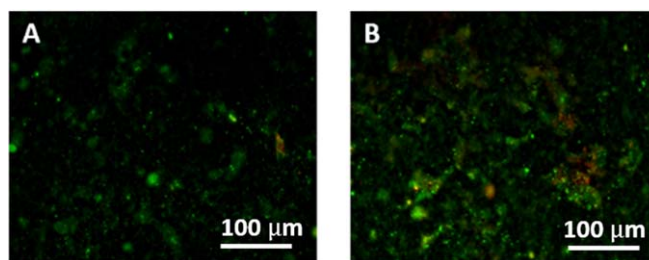


Figure 6. Anodic biofilms observed in fluorescence microscopy using a focus x100 on (A) unmodified SS electrode and (B) CNF-PDMS modified electrode. Biofilms were labelled using a LIVE/DEAD Bactlight viability kit. Dead bacteria with damaged membrane are red, whereas living bacteria with an undamaged membrane are green.

After a month of biofilm growth, the characterization of MFC anodes by fluorescence microscopy showed that the surface of CNF-PDMS/SS electrodes was loaded with a higher coverage percentage of biofilm on a modified surface area than that observed on the unmodified SS electrodes (figure 6). These results indicate that CNF-PDMS layers improved biocompatibility of SS surfaces and the growth of biofilms on this material.

4. Conclusion

Coating of SS anodes with CNF-PDMS layers for MFC application improves the stability of the electrodes for long term power generation. The comb-like conducting structures on CNF-PDMS layers facilitated the direct EET of EAB to the electrode. However, CNF-PDMS coating increase start up period of MFCs probably due to hydrophobic properties of PDMS. The changes in surface characteristics of CNF-PDMS material could improve the interaction between material and bacteria and accelerate biofilm formation. Besides, CNF-PDMS coating had an anti-corrosion effect and enhanced biocompatibility of SS surfaces. This modification method is a promising approach to improve properties of anode materials for MFC application.

Acknowledgments

This work was financially supported by the ‘PHC Utique’ program of the French Ministry of Foreign Affairs and Ministry of higher education, research and innovation and the Tunisian Ministry of higher education and scientific research in the CMCU project number 19MAG23.

ORCID iDs

Naoufel Haddour  <https://orcid.org/0000-0002-2430-5568>

References

- [1] Rabaey K and Keller J 2008 *Water Sci. Technol.* **57** 655–9
- [2] Qiao Y, Bao S J and Li C M 2010 *Energy Environ. Sci.* **3** 544–53
- [3] Li M et al 2018 *Biotechnol. Adv.* **36** 1316–27
- [4] Logan B E, Murano C, Scott K, Gray N D and Head I M 2005 *Water Res.* **39** 942–52
- [5] Wei J, Liang P and Huang X 2011 *Bioresour. Technol.* **102** 9335–44
- [6] Cai H, Wang J, Bu Y and Zhong Q 2013 *J. Chem. Technol. Biotechnol.* **88** 623–8
- [7] Senthilkumar N, Pannipara M, Al-Sehemi A G and Gnana Kumar G 2019 *New J. Chem.* **43** 7743–50
- [8] Yang C et al 2019 *Sci. China Mater.* **62** 645–52
- [9] Zhou M, Chi M, Luo J, He H and Jin T 2011 *J. Power Sources* **196** 4427–35
- [10] Guo K, PrévotEAU A, Patil S A and Rabaey K 2015 *Curr. Opin. Biotech.* **33** 149–56
- [11] Liu H, Cheng S, Huang L and Logan B E 2008 *J. Power Sources* **179** 274–9
- [12] Cheng S, Ye Y, Ding W and Pan B 2014 *J. Power Sources* **248** 931–8
- [13] Guerrini E et al 2014 *J. Electrochem. Soc.* **161** H62–7
- [14] Chen Y et al 2012 *J. Power Sources* **201** 136–41
- [15] Mansfeld F and Little B 1991 *Corrosion Science* **32** 247–72
- [16] Liang Y et al 2017 *J. Power Sources* **342** 98–104
- [17] Pu K B et al 2018 *Biochem. Eng. J.* **132** 255–61
- [18] Ben Slimane A, Chehimi M M and Vaulay M J 2004 *Colloid Polym. Sci.* **282** 314–23
- [19] Bergveld P, Lötters J C, Olthuis W and Veltink P H 1997 *J. Micromechanics Microengineering* **7** 145
- [20] Niu X Z, Peng S L, Liu L Y, Wen W J and Sheng P 2007 *Adv. Mater.* **19** 2682–6
- [21] Cong H and Pan T 2008 *Adv. Funct. Mater.* **18** 1912–21

- [22] Khosla A and Gray B L 2009 *Mater. Lett.* **63** 1203–6
- [23] Gong X and Wen W 2009 *Biomicrofluidics* **3** 012007-14
- [24] Niu X, Zhang M, Peng S, Wen W and Sheng P 2007 *Biomicrofluidics* **1** 1–12
- [25] Brun M, Chateaux J F, Deman A L, Pittet P and Ferrigno R 2011 *Electroanalysis* **23** 321–4
- [26] Cheng S, Liu H and Logan B E 2006 *Electrochem. Commun.* **8** 489–94
- [27] Chu K *et al* 2013 *IEEE Electron Device Lett.* **34** 668–70
- [28] Reguera G *et al* 2006 *Appl. Environ. Microbiol.* **72** 7345–8
- [29] Santoro C *et al* 2014 *Carbon N. Y.* **67** 128–39
- [30] Roy J N, Babanova S, Garcia K E, Cornejo J, Ista L K, Atanassov P *et al* 2014 *Electrochimica Acta* **126** 3–10
- [31] Katuri K P, Rengaraj S, Kavanagh P, O’Flaherty V and Leech D 2012 *Langmuir* **28** 7904–13
- [32] Pinto D, Coradin T and Laberty-Robert C 2018 *Bioelectrochemistry* **120** 1–9